Published in final edited form as:
Cell Stem Cell. 2010 December 5; 7(5): 606–617. doi:10.1016/j.stem.2010.09.013.

Mdm2 is required for survival of hematopoietic stem cells/progenitors via dampening of ROS-induced p53 activity

Hussein A. Abbas[1,2], **Daniela R. Maccio**[2], **Suleyman Coskun**[3], **James G. Jackson**[2], **Amy L. Hazen**[4], **Tiffany M. Sills**[3,5], **M. James You**[6], **Karen K. Hirschi**[3], and **Guillermina Lozano**[1,2,*]

[1] Program in Genes and Development of The Graduate School of Biomedical Sciences, University of Texas Health Science Center, Houston, Texas, 77030, USA

[2] Department of Genetics, University of Texas M. D. Anderson Cancer Center, Houston, Texas, 77030, USA

[3] Department of Pediatrics and Molecular and Cellular Biology; Center for Cell and Gene Therapy; Baylor College of Medicine; Houston, Texas, 77030, USA

[4] Department of Stem Cell Transplant & Cellular Therapy; University of Texas M. D. Anderson Cancer Center, Houston, Texas, 77030, USA

[5] Interdepartmental Program in Cell and Molecular Biology Program; Baylor College of Medicine; Houston, Texas, 77030, USA

[6] Department of Hematopathology, University of Texas M. D. Anderson Cancer Center, Houston, Texas, 77030, USA

Summary

Mdm2 is an E3 ubiquitin ligase that targets p53 for degradation. $p53^{515C}$ (encoding p53R172P) is a hypomorphic allele of *p53* that rescues the embryonic lethality of $Mdm2^{-/-}$ mice. $Mdm2^{-/-}$ $p53^{515C/515C}$ mice, however, die by postnatal day 13 due to hematopoietic failure. Hematopoietic stem cells and progenitors of $Mdm2^{-/-}$ $p53^{515C/515C}$ mice were normal in fetal livers but were depleted in postnatal bone marrows. After birth, these mice had elevated reactive oxygen species (ROS) thus activating p53R172P. In the absence of *Mdm2*, stable p53R172P induced ROS, and cell cycle arrest, senescence and cell death in the hematopoietic compartment. This phenotype was partially rescued with antioxidant treatment and upon culturing of hematopoietic cells in methycellulose at 3% oxygen. p16 was also stabilized due to ROS, and its loss increased cell cycling, and partially rescued hematopoiesis and survival. Thus, *Mdm2* is required to control ROS-induced p53 levels for sustainable hematopoiesis.

Keywords

hematopoietic stem cells; Mdm2; p53; reactive oxygen species; p16

*Correspondence to Guillermina Lozano (gglozano@mdanderson.org), Phone #: 713-834-6386, Fax #: 713-834-6380.

Introduction

Hematopoietic stem cells (HSCs) are the ultimate reservoir that replenish the blood with new cells of all lineages throughout an organism's lifetime (Orkin and Zon, 2008). HSCs emerge at distinct sites throughout development, a journey that is highly conserved among mammalian species. Primitive hematopoiesis and the HSC precursors first appear in the yolk sac at embryonic day (E) 7.5 in the mouse (Palis et al., 1995; Palis et al., 1999). The fetal liver constitutes the major organ for embryonic HSC expansion and definitive hematopoiesis before HSCs engraft the bone marrow and establish it as their major niche throughout the rest of organism's life (Muller-Sieburg et al., 1986).

Reactive oxygen species (ROS) are generated by intrinsic or extrinsic sources, such as oxidative metabolism and ionizing radiation, respectively, and can cause DNA damage (Lombard et al., 2005; Naka et al., 2008). ROS levels distinguish HSC self-renewal capacity. Specifically, HSCs with lower ROS levels can engraft irradiated recipients better than HSCs with higher ROS content (Jang and Sharkis, 2007). Genes involved in ROS-induced DNA damage can also regulate HSC self-renewal. For instance, *Atm* loss induces ROS production by unknown mechanisms, which activates the $p16^{INK4a}$ –retinoblastoma pathway and abrogates HSC self-renewal (Ito et al., 2004; Ito et al., 2006). The hematopoietic phenotype is rescued upon treatment with antioxidants (Ito et al., 2004). Altogether, these studies suggest a strong influence of ROS on HSCs.

p53 is a transcription factor that activates a plethora of genes whose products induce cell cycle arrest, differentiation, senescence, and apoptosis in response to DNA damage signals such as ROS (Ko and Prives, 1996; Vazquez et al., 2008). Mdm2 is an E3 ubiquitin ligase and the major negative regulator of p53 stability (Honda et al., 1997). $Mdm2^{-/-}$ mice die embryonically but nullizygosity of *p53* completely rescues this phenotype (Jones et al., 1995; Montes de Oca Luna et al., 1995). $Mdm2^{-/-}$ $p53^{-/-}$ mice, like $p53^{-/-}$ mice, die by ~8 months of age due to tumor burden, and do not appear to have hematopoietic defects (McDonnell et al., 1999). Additionally, conditional loss of both *Mdm2* alleles in various adult tissues leads to cardiac, intestinal, and lymphoid defects due to constitutively active p53 (Marine et al., 2006).

A rare p53 mutation (Arginine to Proline) in human p53 at amino acid 175 lacks apoptotic activity but still maintains cell cycle arrest activity (Ludwig et al., 1996; Rowan et al., 1996). Our lab previously generated a knock-in $p53^{515C}$ allele in the mouse that encodes p53R172P protein mimicking this human mutation (Liu et al., 2004). Homozygosity of the $p53^{515C}$ allele also rescues the *Mdm2* null phenotype, but $Mdm2^{-/-}$ $p53^{515C/515C}$ mice suffer from hematopoietic defects and succumb to early postnatal mortality (Liu et al., 2007). Restoration of one *Mdm2* allele ($Mdm2^{+/-}$ $p53^{515C/515C}$) completely rescues hematopoiesis and survival. A mechanistic understanding of the role of p53 in hematopoiesis is unclear.

In this study, we show that despite the absence of *Mdm2*, p53R172P is not stabilized during embryogenesis until E18.5 when hematopoiesis proceeds in the bone marrow. HSCs are under higher oxidative stress in the bone marrow than fetal liver stabilizing and activating p53R172P in the bone marrow. Subsequently, p53R172P induced ROS, and cell cycle arrest, senescence and cell death in the hematopoietic compartment of $Mdm2^{-/-}$ $p53^{515C/515C}$ mice. Hematopoiesis was rescued when mice or cells were exposed to lower oxidative stress. Finally, ROS also activated p16, and genetic ablation of *p16* increased bone marrow cycling and cellularity, increased survival, and partially rescued HSCs and progenitors. Thus, oxidative stress was the intrinsic signal that activates p53 in hematopoietic tissues, and HSCs and progenitors are highly sensitive to p53 response. In

summary, Mdm2 is required for survival of HSCs and sustainability of hematopoiesis via downregulation of p53's response to basal ROS levels.

Results

Characterization of the Mdm2$^{-/-}$ p53$^{515C/515C}$ hematopoietic phenotype

Mdm2$^{-/-}$ *p53*$^{515C/515C}$ and *Mdm2*$^{+/-}$ *p53*$^{515C/515C}$ (control) mice were generated from the same litter by breeding *Mdm2*$^{+/-}$ *p53*$^{515C/515C}$ mice to each other. *Mdm2*$^{-/-}$ *p53*$^{515C/515C}$ mice were born at normal Mendelian ratio (Figure 1A) and were indistinguishable from their control littermates at birth. However, by postnatal day (P) 5, *Mdm2*$^{-/-}$ *p53*$^{515C/515C}$ mice became visually discernible from their littermates by their smaller size. All *Mdm2*$^{-/-}$ *p53*$^{515C/515C}$ mice died by P13 (Figure 1A). Analysis of tissues from *Mdm2*$^{-/-}$ *p53*$^{515C/515C}$ neonates revealed severe hematopoietic defects (Figure 1B). Since *Mdm2*$^{-/-}$ *p53*$^{515C/515C}$ were born with no obvious defects, we hypothesized that hematopoiesis was normal during embryogenesis. Indeed, hematoxylin and eosin (H&E) sections of fetal livers at E14.5 and bone marrows at E18.5 confirmed normal cellularity and histology compared to *Mdm2*$^{+/-}$ *p53*$^{515C/515C}$ littermate controls (Figure 1B). By P6, bone marrow cellularity begins to fall to 60%–70% of control. The bone marrow becomes almost acellular at P10 (<10% cellularity) (Figure 1B).

Since Mdm2 targets p53 for degradation, we performed immunohistochemisty (IHC) on hematopoietic tissues at various time points to investigate p53R172P levels. E14.5 fetal livers of *Mdm2*$^{+/-}$ *p53*$^{515C/515C}$ and *Mdm2*$^{-/-}$ *p53*$^{515C/515C}$ mice had very low levels of p53R172P staining and were indistinguishable (Figure 1C). On the other hand, bone marrow cells of *Mdm2*$^{-/-}$ *p53*$^{515C/515C}$ mice had elevated p53R172P staining at E18.5, P6, P8 and P10. Control *Mdm2*$^{+/-}$ *p53*$^{515C/515C}$ littermates were negative for p53R172P at all time points except for a few p53R172P positively stained cells (Figure 1C). Hence, high p53R172P levels correlated with decreased bone marrow cellularity. This phenotype is p53R172P dependent as deletion of one *p53* allele rescues the early postnatal lethality (Liu et al., 2007). We repeated these crosses and observed that *Mdm2*$^{-/-}$ *p53*$^{-/515C}$ mice were born at the correct Mendelian ratio. *Mdm2*$^{-/-}$ *p53*$^{-/515C}$ mice were sacrificed at 6 months of age without further analysis. In all assays (see below), *Mdm2*$^{+/-}$ *p53*$^{515C/515C}$ were indistinguishable from Mdm2$^{+/+}$ p53$^{515C/515C}$ mice.

p53R172P activated cell cycle inhibitors and to a lesser extent apoptotic targets in postnatal bone marrows

While E14.5 fetal livers showed normal histology and no p53R172P staining, P6 moribund mice had stable p53R172P levels (Figures 1B–C). Most importantly, P6 bone marrows maintained 60–70% bone marrow cellularity (Figure 1B) providing us with enough cells for mechanistic studies. Hence, we chose E14.5 fetal livers and P6 bone marrows as representative time points for detailed molecular characterization of the embryonic and neonatal phenotypes, respectively. We isolated RNA from whole fetal livers at E14.5 and examined cell cycle arrest targets of p53: *p21* and *Ccng*. *p21* and *Ccng* mRNA levels were not significantly different between *Mdm2*$^{-/-}$ *p53*$^{515C/515C}$ and control Mdm2$^{+/-}$ *p53*$^{515C/515}$ fetal livers (Figure S1A). We also examined the apoptosis targets of p53 and found no differences in induction of *Noxa*, *Perp*, or *Puma* in fetal livers of *Mdm2*$^{-/-}$ *p53*$^{515C/515C}$ compared to *Mdm2*$^{+/-}$ *p53*$^{515C/515C}$ mice (Figure S1A). On the other hand, all *Mdm2*$^{-/-}$ *p53*$^{515C/515C}$ whole bone marrows at P6 had dramatic and significant induction of p53 cell cycle targets *Ccng* (9 fold) and *p21* (43 fold) compared to control *Mdm2*$^{+/-}$ *p53*$^{515C/515C}$ littermates (Figure 2A). As for apoptotic targets, *Puma* and *Noxa* levels were consistently two fold higher in *Mdm2*$^{-/-}$ *p53*$^{515C/515C}$ moribund mice than in *Mdm2*$^{+/-}$ *p53*$^{515C/515C}$ mice ($p<0.02$) (Figure 2A). *Perp* levels were the same in all mice (Figure 2A).

Increased senescence in Mdm2$^{-/-}$ p53$^{515C/515C}$ P6 bone marrows

p53R172P protein also induces senescence in several mouse models (Cosme-Blanco et al., 2007; Post et al., 2009). We therefore hypothesized that *Mdm2*$^{-/-}$ *p53*$^{515C/515C}$ bone marrows in early postnatal development may also exhibit a senescent phenotype. Accordingly, in addition to *p21*, we examined expression levels of other senescent markers *Dcr2, p15, p16, Dec1 and Pml* using RT-PCR (Collado et al., 2005; Collado and Serrano, 2006). Expression levels of these genes in E14.5 whole fetal liver cells were the same between *Mdm2*$^{-/-}$ *p53*$^{515C/515C}$ embryos and controls (Figure S1B). In P6 bone marrows, *p21* (43 fold), *Dcr2* (17 fold) and *p15* (11 fold) were highly elevated in *Mdm2*$^{-/-}$ *p53*$^{515C/515C}$ mice as compared to controls, while *Dec1*, *p16* and *Pml* mRNA levels did not change (Figure 2B). We next examined senescence associated β-galactosidase (SA-β-gal) activity in freshly isolated postnatal bone marrow cells. Approximately 11% of *Mdm2*$^{-/-}$ *p53*$^{515C/515C}$ cells were positive for SA-β-gal compared to less than 5% for control littermates (p=0.0071) (Figure 2C and S1C).

Decreased cycling and increased cell death in postnatal bone marrows of Mdm2$^{-/-}$ p53$^{515C/515C}$

To investigate the cell cycle pattern in fetal livers and postnatal bone marrows, we fixed cells from these tissues and analyzed for DNA content. Cell cycle patterns of E14.5 fetal livers between *Mdm2*$^{-/-}$ *p53*$^{515C/515C}$ and *Mdm2*$^{+/-}$ *p53*$^{515C/515C}$ littermates were indistinguishable as expected (Figure 2D). Specifically, 53%, 28% and 16% of whole fetal liver cells in *Mdm2*$^{-/-}$ *p53*$^{515C/515C}$ embryos were in G1, S, G2/M phase similar to 53%, 27% and 16% in control *Mdm2*$^{+/-}$ *p53*$^{515C/515C}$ littermates (Figure 2D). The fraction of cells in subG1 was less than 2% in both genotypes (Figure 2D).

P6 bone marrows, however, showed significant differences between the two genotypes. Less than 6.5% of *Mdm2*$^{-/-}$ *p53*$^{515C/515C}$ bone marrow cells were in S phase compared to 22% of control littermates (Figure 2E). *Mdm2*$^{-/-}$ *p53*$^{515C/515C}$ neonates had 7% of cells in G2/M compared to 13% in *Mdm2*$^{+/-}$ *p53*$^{515C/515C}$ littermates (Figure 2E). A significant percentage of *Mdm2*$^{-/-}$ *p53*$^{515C/515C}$ bone marrow cells (15%) as compared to <1% of control bone marrow cells were in subG1 fraction suggesting cell death as another mechanism of depleting the cellular compartment (Figure 2E).

Since *Puma* and *Noxa* were elevated in *Mdm2*$^{-/-}$ *p53*$^{515C/515C}$ P6 bone marrows, and since 15% of these cells were in subG1, we investigated apoptosis as a mechanism for depleting hematopoiesis. Except for a few positive cells, caspase-3 staining was negative in all bone marrows at P6 and P8 by IHC (Figure 2F). We then used Annexin V staining as an alternative method to examine apoptosis. E14.5 whole fetal livers and P6 whole bone marrows of both *Mdm2*$^{-/-}$ *p53*$^{515C/515C}$ and *Mdm2*$^{+/-}$ *p53*$^{515C/515C}$ pups had less than 6% Annexin V positive cells and differences between genotypes were statistically insignificant (Figures S1D-E). Hence, although cell death is occurring, the standard markers for apoptosis are negative suggesting an alternative mechanism of cell death.

p21 loss does not rescue hematopoiesis but extends lifespan of Mdm2$^{-/-}$ p53$^{515C/515C}$ mice

p21 expression levels were the highest in *Mdm2*$^{-/-}$ *p53*$^{515C/515C}$ bone marrows among all genes tested at P6 (Figure 2A). Also, *p21* maintains quiescence in HSCs (Cheng et al., 2000). Hence, we hypothesized that *p21* deletion might rescue hematopoiesis by increasing proliferation and alleviating senescence of bone marrows. Contrary to our expectations, however, *Mdm2*$^{-/-}$ *p53*$^{515C/515C}$ *p21*$^{-/-}$ mice suffered from acellular bone marrows and succumbed to growth retardation (data not shown). However, the median age and life expectancy were longer for these mice indicating a partial rescue of postnatal lethality

(Figure S1F). Increased survival may be due to effects on other tissues as *Mdm2*$^{-/-}$ *p53*$^{515C/515C}$ mice also suffer from multiple defects (Liu et al., 2007).

Defective HSC and progenitor populations in bone marrows of Mdm2$^{-/-}$ p53$^{515C/515C}$ mice

HSCs are responsible for replenishing the cellular compartment of the blood. Since *Mdm2*$^{-/-}$ *p53*$^{515C/515C}$ bone marrows reflect absence of sustainable hematopoiesis, we hypothesized a defect in the HSC and progenitor populations. We therefore examined Lin – ckit+ Sca1+ (LKS) and Lin – ckit+ Sca1–/low cell populations that represent HSCs and common lymphoid and myeloid progenitors (CLP/CMP), respectively, at different time points (Morrison and Weissman, 1994; Weissman and Shizuru, 2008).

E14.5 fetal livers of *Mdm2*$^{-/-}$ *p53*$^{515C/515C}$ and *Mdm2*$^{+/-}$ *p53*$^{515C/515C}$ mice had normal LKS cell populations (0.236% and 0.24%) for *Mdm2*$^{+/-}$ *p53*$^{515C/515C}$ and *Mdm2*$^{-/-}$ *p53*$^{515C/515C}$ embryos, respectively and normal CLP/CMP populations (5.26% and 5.58%) for *Mdm2*$^{+/-}$ *p53*$^{515C/515C}$ and *Mdm2*$^{-/-}$ *p53*$^{515C/515C}$ embryos, respectively (Figures 3A–B). This was expected given the normal histology, absence of p53R172P stability, and normal cell cycle of fetal livers at E14.5. However, E18.5 bone marrows of *Mdm2*$^{-/-}$ *p53*$^{515C/515C}$ embryos showed significant decreases in LKS and CLP/CMP populations. Specifically, 0.117% and 0.508% of whole bone marrow cells are LKS and CLP/CMP populations, respectively, in *Mdm2*$^{-/-}$ *p53*$^{515C/515C}$ compared to 0.474% and 1.74%, respectively, in *Mdm2*$^{+/-}$ *p53*$^{515C/515C}$ littermates at E18.5 (Figures 3A–B).

Postnatally, the differences were even more pronounced. Specifically, at P4, LKS (0.044% in *Mdm2*$^{-/-}$ *p53*$^{515C/515C}$ vs. 0.243% in control) and CLP/CMP (0.273% in *Mdm2*$^{-/-}$ *p53*$^{515C/515C}$ vs. 1.726% in control) populations were dramatically low in bone marrows of *Mdm2*$^{-/-}$ *p53*$^{515C/515C}$ mice (Figures 3A–B). At P6, LKS and CLP/CMP levels dropped further to <0.0103% and <0.075% of whole bone marrows, respectively, while control *Mdm2*$^{+/-}$ *p53*$^{515C/515C}$ consistently had significant higher levels (0.265% for LKS and 1.292% for CLP/CMP of whole bone marrow) (Figures 3A–B). These populations became almost extinct by P8 in *Mdm2*$^{-/-}$ *p53*$^{515C/515C}$ mice (Figures 3A–B).

To further enrich for HSCs, we used two additional markers (CD48 and CD150) with LKS, hereafter referred to as SLAM-LKS (Kiel et al., 2005; Kim et al., 2006). 0.042% of *Mdm2*$^{-/-}$ *p53*$^{515C/515C}$ fetal liver cells at E14.5 were SLAM-LKS while 0.036% for *Mdm2*$^{+/-}$ *p53*$^{515C/515C}$ controls (p=0.69) again indicating no differences at this embryonic stage (Figures 3C). P6 whole bone marrows showed >2 fold decrease in the SLAM-LKS population in *Mdm2*$^{-/-}$ *p53*$^{515C/515C}$ (0.02%) bone marrows as compared to *Mdm2*$^{+/-}$ *p53*$^{515C/515C}$ controls (0.047%) (p=0.02) (Figures 3D). Thus, regardless of mode for enriching for HSCs, this population was decreased in bone marrows of *Mdm2*$^{-/-}$ *p53*$^{515C/515C}$ pups as compared to controls.

Ex vivo culture at 20% oxygen shows absence of hematopoiesis during embryonic and postnatal development

To evaluate HSCs and CLP/CMP differentiation capacity *ex vivo*, we used methylcellulose cultures. Colonies are identified based on morphology. Specifically, we looked for burst-forming unit erythroid (BFU-E), colony-forming unit granulocyte macrophage (CFU-GM) and colony-forming unit granulocyte erythroid monocyte and megakaryocyte (GEMM) colonies. *Mdm2*$^{-/-}$ *p53*$^{515C/515C}$ E9.5 yolk sacs, E14.5 fetal livers, and P2 bone marrows showed no hematopoietic activity *ex vivo*, while the same tissues from control *Mdm2*$^{+/-}$ *p53*$^{515C/515C}$ littermates grew well in culture (Figures 3E–F and S2). Noteworthy, E14.5 fetal liver and P2 bone marrow of *Mdm2*$^{+/+}$ *p53*$^{515C/515C}$ hematopoietic activity in methocult showed no significant differences for all lineages compared to *Mdm2*$^{+-}$

p53$^{515C/515C}$ (Figures 3E–F). Thus, the *ex vivo* assays did not reproduce our *in vivo* results showing normal LKS and CLP/CMP populations in *Mdm2*$^{-/-}$ *p53*$^{515C/515C}$ fetal livers. These differences suggested oxidative stress as an impediment for growth.

ROS levels are high in Mdm2$^{-/-}$ p53$^{515C/515C}$ bone marrows

ROS are major sensitizers of the hematopoietic system (Naka et al., 2008). Whether ROS effects are mediated via the p53 pathway in the hematopoietic compartment is unknown. To examine ROS levels in fetal livers and postnatal bone marrows, we used 5-(and-6)-carboxy-2′,7′-dichlorofluorescein diacetate (DCFDA). We chose E14.5 fetal liver and P6 bone marrow as representative embryonic and postnatal time points, respectively. ROS levels of whole fetal livers and LKS populations at E14.5 between *Mdm2*$^{+/-}$ *p53*$^{515C/515C}$ and *Mdm2*$^{-/-}$ *p53*$^{515C/515C}$ mice were not statistically different (Figures 4A–B).

Postnatally, mice are exposed to atmospheric oxygen levels. Indeed, *Mdm2*$^{+-}$ *p53*$^{515C/515C}$ whole bone marrows and LKS populations had 3.8 and 1.5 times more ROS, respectively, compared to the same populations in E14.5 fetal livers (Figure 4A–B). This indicated that ROS levels within the hematopoietic compartment were higher postnatally.

Since all pups are littermates, we expected that ROS levels of *Mdm2*$^{+/-}$ *p53*$^{515C/515C}$ and *Mdm2*$^{-/-}$ *p53*$^{515C/515C}$ littermates to be the same at P6. To our surprise, *Mdm2*$^{-/-}$ *p53*$^{515C/515C}$ pups had 3.3 times higher ROS levels in whole bone marrow compared to control (Figure 4A). ROS were also higher in E18.5 bone marrows as compared to fetal livers regardless of genotype (Figure S3A). ROS levels in the LKS population of *Mdm2*$^{-/-}$ *p53*$^{515C/515C}$ pups was consistently 3 fold (p=0.005) higher than *Mdm2*$^{+/-}$ *p53*$^{515C/515C}$ littermates in P6 bone marrows (Figures 4B and S3B). The CLP/CMP population of *Mdm2*$^{-/-}$ *p53*$^{515C/515C}$ pups at P6 also had 3.6 fold (p=0.0009) higher ROS than control *Mdm2*$^{+/-}$ *p53*$^{515C/515C}$ pups (Figure 4C). These data show that *Mdm2*$^{-/-}$ *p53*$^{515C/515C}$ bone marrows generated more ROS in LKS and CLP/CMP populations.

We next investigated whether elevated ROS in postnatal bone marrows compared to fetal livers was due to temporal (embryonic vs. postnatal) or spatial (liver vs. bone marrow) differences. P6 livers and bone marrows of *Mdm2*$^{+/-}$ *p53*$^{515C/515C}$ and *Mdm2*$^{-/-}$ *p53*$^{515C/515C}$ pups examined had similar ROS levels in their livers compared to bone marrows of same mice at P6 (Figure 4D). These data clearly demonstrated that the differences seen in ROS between fetal livers and postnatal bone marrows were due to temporal variation and not the bone marrow niche *per se*.

Increased expression of ROS inducing genes in Mdm2$^{-/-}$ p53$^{515C/515C}$ pups

To address what instigated higher rates of ROS in P6 bone marrows of *Mdm2*$^{-/-}$ *p53*$^{515C/515C}$ mice compared to controls, we examined p53's role in ROS. p53 can transactivate a set of ROS-inducing genes dubbed p53-induced-genes (PIG) which lead to cell death (Polyak et al., 1997). Specifically, we examined mRNA levels of *Pig1*, *Pig8* and *Pig12*, the most highly induced *Pig* genes (Polyak et al., 1997). *Pig1* is a member of galectin family that can stimulate superoxide production (Yamaoka et al., 1995). *Pig8* is induced following etoposide treatment and is known to generate ROS (Lehar et al., 1996). *Pig12* is a microsomal glutathione transferase homologue and is involved in redox reactions (Lee and DeJong, 1999).

At P6, *Pig1* and *Pig8* levels were 2 (p=0.01) and 3 (p<0.0001) fold higher in *Mdm2*$^{-/-}$ *p53*$^{515C/515C}$ bone marrows as compared to control littermates (Figure 4E). *Pig12* levels were the same at P6. Since p53 activates *Pig* genes in a cascading manner, we examined expression of these genes in P10 whole bone marrows as well. *Pig12* levels at P10 were 2.8 fold higher (p=0.01) in moribund *Mdm2*$^{-/-}$ *p53*$^{515C/515C}$ mice as compared to control

littermates (Figure 4F). *Pig1* (p=0.49) and *Pig8* (p=0.07) levels were not statistically different at P10 (Figure 4F).

NAC injections partially rescue HSC and CLP/CMP at P6 in vivo

N-acetyl Cysteine (NAC) is an anti-oxidant. Since $Mdm2^{-/-}$ $p53^{515C/515C}$ mice lose their HSCs and die by P13, we injected pups at P3 and P5 with NAC. Unfortunately, this technique was highly invasive and most pups of all genotypes died after the first injection. However, two $Mdm2^{+/-}$ $p53^{515C/515C}$ and two $Mdm2^{-/-}$ $p53^{515C/515C}$ pups survived and were sacrificed at P6 to examine HSC and CLP/CMP populations. A modest but significant increase in both of these populations was prominent in $Mdm2^{-/-}$ $p53^{515C/515C}$ pups injected with NAC compared to untreated mice of same genotype (Figures 5A–B). Specifically, there was a ~4 fold (p=0.001) increase in LKS population of whole bone marrow and 7 fold (p=0.01) increase in CLP/CMP population of whole bone marrow in treated versus untreated mice (Figures 5A–B). The two $Mdm2^{+/-}$ $p53^{515C/515C}$ pups treated with NAC that survived had no significant differences in HSC and CLP/CMP populations compared to untreated genotype-matched mice (Figures 5A–B). Notably, a third $Mdm2^{-/-}$ $p53^{515C/515C}$ mouse that survived two injections of NAC, received a third injection at P7, and was sacrificed at P10. Bone marrow cellularity was ~80% restored in the treated mouse compared to the $Mdm2^{-/-}$ $p53^{515C/515C}$ untreated control (Figure 5C).

These data suggest that ROS contributes to the hematopoietic defect in $Mdm2^{-/-}$ $p53^{515C/515C}$ mice. Our initial *ex vivo* assays were performed at 20% oxygen. We therefore examined hematopoiesis *ex vivo* at 3% oxygen levels. Specifically, cells from E14.5 fetal livers and P2 bone marrows of the same pups used in Figures 3C–D were plated onto methycellulose. Contrary to culturing in 20% oxygen, 3% oxygen levels allowed hematopoiesis to proceed unimpeded and all $Mdm2^{-/-}$ $p53^{515C/515C}$ tissues formed CFU-GM, BFU-E and GEMM indistinguishable from controls $Mdm2^{+/-}p53^{515C/515C}$ (Figures 5D–E). Hence, all $Mdm2^{-/-}$ $p53^{515C/515C}$ fetal livers and P2 bone marrows examined showed complete rescue of hematopoiesis in methylcellulose cultures at 3% oxygen. These data indicate that oxidative stress was the major impediment for sustainable hematopoiesis in the absence of *Mdm2* due to activation of p53R172P.

WBM of P6 $Mdm2^{-/-}$ $p53^{515C/515C}$ mice cannot rescue lethally irradiated mice

To measure reconstitution capacity of $Mdm2^{-/-}$ $p53^{515C/515C}$ HSCs, we transplanted $0.5x10^6$ whole bone marrow cells from CD45.2 P6 $Mdm2^{+/}p53^{515C/515C}$ and $Mdm2^{-/-}$ $p53^{515C/515C}$ pups into lethally irradiated CD45.1 congenic mice and monitored survival and engraftment. Eight of eight mice transplanted with $Mdm2^{+/-}$ $p53^{515C/515C}$ WBM survived at least 45 days (end point of the experiment), while 8/8 mice transplanted with $Mdm2^{-/-}$ $p53^{515C/515C}$ died within 12 days post lethal irradiation (Figure 5F). Surviving mice had at least 85% donor derived (CD45.2) cells confirming that P6 WBM of $Mdm2^{+/-}$ $p53^{515C/515C}$ can engraft and reconstitute hematopoiesis for lymphoid and myeloid lineages (Figures 5G and S4A–D). We then supplemented NAC in drinking water of another cohort of recipient mice to address whether antioxidant treatment could rescue $Mdm2^{-/-}$ $p53^{515C/515C}$ HSC activity. Five of five recipient mice transplanted with $Mdm2^{-/-}$ $p53^{515C/515C}$ WBM and provided with NAC did not survive (Figure 5F).

p16 deletion partially rescues bone marrow cellularity and extends survival of $Mdm2^{-/-}$ $p53^{515C/515C}$ mice

p16 is activated due to ROS (Ito et al., 2004). Since ROS levels were elevated in $Mdm2^{-/-}$ $p53^{515C/515C}$ bone marrows, we examined p16 status. Although *p16* mRNA levels were indistinguishable between $Mdm2^{-/-}$ $p53^{515C/515C}$ and control littermates at P6 (Figure 2B), we detected significantly elevated p16 protein levels by IHC at P6, P8 and P10 and by

immunofluorescence at P8 in *Mdm2*$^{-/-}$ *p53*$^{515C/515C}$ bone marrows using two different antibodies (Figures 6A–B). Bone marrows of control *Mdm2*$^{+/-}$ *p53*$^{515C/515C}$ littermates had some positive cells for p16 staining but much less than *Mdm2*$^{-/-}$ *p53*$^{515C/515C}$ mice (Figures 6A–B).

To address whether *p16* deletion can restore hematopoiesis, we generated *Mdm2*$^{+/-}$ *p53*$^{515C/515C}$ *p16*$^{-/-}$ mice and crossed them to each other. Although these mice were smaller than normal and their pregnancy rate was low, they were still able to generate pups. Three *Mdm2*$^{-/-}$ *p53*$^{515C/515C}$ *p16*$^{-/-}$ mice from two independent crosses sacrificed at P10 (where bone marrow acellularity is most dramatic in *Mdm2*$^{-/-}$ *p53*$^{515C/515C}$ mice) showed restoration of bone marrow cellularity by at least 80% (Figures 6C–D). Also, *Mdm2*$^{-/-}$ *p53*$^{515C/515C}$ *p16*$^{-/-}$ mice lived significantly ($p<0.0001$) longer than *Mdm2*$^{-/-}$ *p53*$^{515C/515C}$ mice (Figure 6E).

Mdm2$^{-/-}$ p53$^{515C/515C}$ p16$^{-/-}$ bone marrows have increased LKS and CLP/CMP populations compared to Mdm2$^{-/-}$ p53$^{515C/515C}$ bone marrows

In order to examine the mechanism behind rescue of bone marrow cellularity upon genetic deletion of *p16*, we first examined p53R172P levels in *Mdm2*$^{-/-}$ *p53*$^{515C/515C}$ *p16*$^{-/-}$ bone marrows by IHC at P10. p53R172P was still high in *Mdm2*$^{-/-}$ *p53*$^{515C/515C}$ *p16*$^{-/-}$ bone marrows (Figure 7A). We then examined the cell cycle status of *Mdm2*$^{-/-}$ *p53*$^{515C/515C}$ *p16*$^{-/-}$ bone marrows at P6. The fraction of cells in *Mdm2*$^{-/-}$ *p53*$^{515C/515C}$ *p16*$^{-/-}$ bone marrows that were in S phase was two fold higher (12.9%) than bone marrows of *Mdm2*$^{-/-}$ *p53*$^{515C/515C}$ mice (6.5%) (Figure 7B). The subG1 population in *Mdm2*$^{-/-}$ *p53*$^{515C/515C}$ *p16*$^{-/-}$ bone marrows was not significantly different from *Mdm2*$^{-/-}$ *p53*$^{515C/515C}$ bone marrows. This indicated that increased bone marrow cycling contributed to rescue of bone marrow cellularity.

We then analyzed the LKS and CLP/CMP populations of *Mdm2*$^{-/-}$ *p53*$^{515C/515C}$ *p16*$^{-/-}$ mice compared to *Mdm2*$^{-/-}$ *p53*$^{515C/515C}$ bone marrows at P6. There was a significant increase in both of these populations. Specifically, LKS populations increased by 4 fold to 0.0413% in whole bone marrow upon deletion of *p16* compared to 0.0103% in *Mdm2*$^{-/-}$ *p53*$^{515C/515C}$ mice (Figure 7C). CLP/CMP levels increased 9 fold upon deletion of *p16* and reached 0.686% of whole bone marrow (Figure 7D). Although LKS and progenitor levels did not return to normal levels as in *Mdm2*$^{+/-}$ *p53*$^{515C/515C}$ mice, this increase was consistent and can explain the replenishment of bone marrow cellularity at P10 (Figure 6C). *Mdm2*$^{+/-}$ *p53*$^{515C/515C}$ *p16*$^{-/-}$ bone marrows had no significant changes in LKS or CLP/CMP populations compared to *Mdm2*$^{+/-}$ *p53*$^{515C/515C}$ bone marrows (Figures 7C–D).

Discussion

Mdm2 is a potent inhibitor of p53 activity. Loss of *Mdm2* in mice leads to an embryo lethal phenotype that is p53-dependent (Jones et al., 1995; Montes de Oca Luna et al., 1995). Tissue specific deletion of *Mdm2* and studies with hypomorphic alleles have shed light on the importance of maintaining low p53 levels in numerous adult tissues as well (Marine et al., 2006; Mendrysa et al., 2003; O'Leary et al., 2004; Ringshausen et al., 2006; Zafon, 2007). In this study, we utilized the *p53*^{515C} hypomorphic allele which in an *Mdm2*-null background leads to severe hematopoietic defects that occur postnatally. In this model, the p53R172P protein is activated in bone marrows at late embryogenesis and postnatally, but not in fetal livers by E14.5 suggesting intrinsic signals activate p53 in a tissue specific manner. p53R172P activity impeded hematopoiesis via induction of cell cycle arrest, senescence, and ultimately cell death in HSCs and progenitors. The defect seen in *Mdm2*$^{-/-}$ *p53*$^{515C/515C}$ HSCs is intrinsic as these cells failed to rescue lethally irradiated wild type mice. This hematopoietic defect is p53-dependent as loss of a single *p53*^{515C} allele

completely rescues the phenotype. In other models, wild type p53 also causes hematopoietic defects emphasizing the relevance of studying our model (Terzian et al., 2007). Thus, Mdm2 functions as a major contributor to keeping p53 levels low. In contrast, HSCs lacking *p53* exit quiescence and show increased cycling (Liu et al., 2009). Balancing p53 levels is thus crucial for cellular homeostasis.

Several studies suggest a direct role of ROS in regulation of HSC fate. For instance, ATM-mediated inhibition of oxidative stress maintains HSC self-renewal capacity (Ito et al., 2004). In *Drosophila*, higher ROS levels sensitize common myeloid progenitors to differentiation (Owusu-Ansah and Banerjee, 2009). We therefore examined ROS levels as a possible intrinsic signal for activation of p53 and showed that whole bone marrows and HSCs had increased ROS levels as compared to fetal livers possibly due to accumulation of ROS from metabolic products during development and direct exposure to atmospheric oxygen. Increased ROS have also been implicated in cellular senescence as observed in our mouse model (Chen et al., 1995). Notably, the hematopoietic defect was rescued *ex vivo* at lower oxygen culture conditions and *in vivo* by antioxidant treatment. However, HSCs from $Mdm2^{-/-}$ $p53^{515C/515C}$ mice did not rescue lethally irradiated recipients supplemented with NAC possibly because ROS levels were too high for the dose of NAC used. Other studies have shown p16 activation due to ROS in bone marrows (Ito et al., 2004; Liu et al., 2009). *p16* deletion rescues hematopoiesis by inducing higher cell cycling providing the first genetic evidence for a direct link of ROS, p16 and hematopoiesis. Importantly, *p16* loss does not decrease p53 levels implying that p16 functions in a complementary pathway.

Although $Mdm2^{-/-}$ $p53^{515C/515C}$ and $Mdm2^{+/-}$ $p53^{515C/515C}$ pups were littermates, the former bone marrows showed significantly higher ROS levels than the latter at postnatal time points. p53 directly induces production of ROS via transactivation of *Pig* genes (Polyak et al., 1997). The *Pig* genes were also elevated in this model creating a positive feedback loop and abrogating HSC function (Figure 7E). Since other studies clearly demonstrate that wild type p53 can transactivate ROS-inducing genes (Donald et al., 2001; Li et al., 1999; Polyak et al., 1997), we believe that the ROS-production in $Mdm2^{-/-}$ $p53^{515C/515C}$ bone marrows is due to normal function of p53R172P. Notably, elevated ROS in P6 bone marrows was not due to bone marrow niche *per se* but more probably due to temporal accumulation of ROS.

In summary, our study sheds light on the importance of the p53-Mdm2 pathway in hematopoiesis. In our model, basal ROS levels accumulate in hematopoietic tissues during development. Normally, the balance between Mdm2 and p53 is highly regulated. In the absence of *Mdm2* and in the presence of basal oxidative stress, p53 activity increases. p53 instigates further ROS production via transactivation of PIGs, creating a positive feedback loop (Figure 7E). These processes deplete HSCs and progenitors via induction of cell cycle arrest, senescence, and ultimately cell death. Hence, caution is warranted when treating patients with p53 reactivating drugs and/or Mdm2-p53 binding inhibitors as such drugs can affect the hematopoietic compartment and deplete hematopoietic stem cells/progenitors. In contrast though, sensitization of bone marrows and HSCs to the ROS-p53 pathway can be exploited in leukemias as leukemia stem cells can arise from HSCs and both share several characteristics (Passegue et al., 2003). Thus, even during normal hematopoiesis, p53 is activated by stress signals, and *Mdm2* is required to regulate p53 levels and allow stem cell survival.

Experimental procedures

Mice

We used previously described $Mdm2^{+/-}$ (Montes de Oca Luna et al., 1995) and $p53^{515C/515C}$ (Liu et al., 2004) mice. $Mdm2^{+/-}$ $p53^{515C/515C}$ mice were bred to each other to generate $Mdm2^{-/-}$ $p53^{515C/515C}$, $Mdm2^{+/+}$ $p53^{515C/515C}$ and $Mdm2^{+/-}$ $p53^{515C/515C}$ littermates. All mice were at >90% C57BL/6 background as determined by marker analysis by Genetic Services at MDACC. Genotyping was performed as previously described for $p53^{515C}$ (Liu et al., 2004), Mdm2 (Montes de Oca Luna et al., 1995), p16 (Sharpless et al., 2001) and p21 (Brugarolas et al., 1998). For antioxidant injections, NAC (A7250, Sigma-Aldrich, MO, USA) was prepared in phosphate buffered saline and injected at P3 and P5 at 1mg/g using a 28 gauge needle around the groin region. Pups were sacrificed at P6. All animal studies were approved by the Institutional Animal Care and Use Committee.

Histology and immunostaining of hematopoietic tissues

Pregnant females were sacrificed at designated time points. Neonates were decapitated. Tissues were either fixed in formalin for 48 hours then paraffin embedded for histological studies, or processed for RNA isolation and stem cell analysis. For tissues, slides were sectioned at 6 μm and stained with Hematoxylin & Eosin by the Department of Veterinary Medicine and Surgery Histology Service at MDACC. Antibodies used were: p53 (#CM5, Vector Laboratories, CA, USA) at 1:500, p16 (#M-156, Santa Cruz Biotechnology, CA, USA) at 1:50 and cleaved caspase-3 (#9661, Cell Signaling, MA, USA) at 1:200 as previously described (Post et al., 2009). For p16 immunofluorescence, we used p16 conjugated to Alexa Fluor® 647 (#F-12, Santa Cruz Biotechnology, CA, USA).

SA-βgal assay

Whole bone marrows from P6-P8 bone marrows were collected and cytospun on slides. Cells were stained with Senescence β-Galactosidase Staining Kit (#9860, Cell Signaling, MA, USA) according to manufacturer's protocol. The number of blue cells were counted in 6 random fields and averaged.

RNA analysis

Bone marrows were homogenized and RNA was extracted using TRIzol (#155-96-026, Invitrogen, MD, USA) and treated with DNase (#04716728001, Roche, IN, USA) as previously described (Jackson and Pereira-Smith, 2006). First-strand DNA was generated by using First-strand cDNA synthesis kit from (#27-9261-01, GE Healthcare, NJ, USA). For Figures 2A, 2B, 4E and 4F bone marrows from two littermates of the same genotype were combined to provide an adequate amount of tissue to produce sufficient RNA for analysis. Primer sequences are in Supplementary Table 1. All levels were normalized to *Gapdh*.

Tissue homogenization and flow cytometry

Tissues were washed with Hanks' Balanced Salt Solution (#21-022-CV, Mediatech, Inc., VA, USA) supplemented with 2% Fetal Bovine Serum (#S11150, Atlanta Biologicals, GA, USA), 10mM Hepes Buffer (#25-060, Mediatech, Inc., VA, USA) and 1x Penicillin-streptomycin solution (#30–002, Mediatech, Inc., VA, USA), termed HBSS+. Cells were kept in Dulbecco's Modified Eagle Medium (DMEM) (#10-107, Mediatech, Inc., VA, USA) with supplements as described for HBSS+. Fetal livers were homogenized with 181/2 G needle and passed through a 40 μm filter (#342340, BD Falcon, NJ, USA). Bones from fore limbs were cleaned of muscle and cartilage, and marrows were finely chopped and filtered as above. For flow cytometry, murine HSC and MPP were identified using eBioscience (CA, USA) fluorochrome conjugated antibodies against ckit (PE_Cy7), Sca-1 (APC), and

for lineage depletion we used CD4 (PE), CD8a (PE), B220 (PE), Ter119 (PE) and Gr-1 (PE) in HBSS+. For SLAM-LKS analysis, Lineage and Sca-1 markers were used as described above (conjugated to PE amd APC, respectively). We also included CD48-PE (#12-0481, eBioscience, CA, USA), ckit-APC_CH7 (#560185, BDBioscience, NJ, USA) and CD150-PE_Cy7 (#115914, Biolegend, CA, USA). Cells were stained for 20 minutes in the dark on ice then washed with HBSS+ before analysis on BD LSRII System at MDACC Flow Cytometry Core Facility. Dead cells were excluded with 7AAD or DAPI staining (eBioscience, CA, USA). For ROS levels, cells were incubated with H_2DCFDA (D-399, Invitrogen, MD, USA) at 37^{o}C in the dark for 20 minutes at a final concentration of 1nM after LKS or CLP/CMP staining. Cells were then washed and kept to recover for 20 minutes at 37^{o}C in the dark.

Cell cycle and Annexin V analysis

Tissues were fixed with 70% ethanol and kept at 4° until stained with propidium iodide (#P3566, Invitrogen, MD, USA). Samples were analyzed on BD FACSCalibur System. Fetal livers and bone marrows were stained with FITC-conjugated Annexin V using ApoAlert Annexin V Apoptosis Kit (#630109, Clontech, CA, USA) according to manufacturer's protocol. Data were analyzed on FlowJo.

Transplantation experiments

C57/B6 CD45.1+ mice were irradiated with a split dose of 5.5 Gy 4 hours apart. Two hours after the second dose, 0.5x10^6 whole bone marrow cells from P6 *Mdm2*$^{-/-}$ *p53*$^{515C/515C}$ and *Mdm2*$^{+/-}$ *p53*$^{515C/515C}$ mice were injected retroorbitally into isofluorane-sedated mice. Mice were monitored for survival on daily basis. For irradiation control, two mice were irradiated without transplantation for each experiment. For engraftment analysis, mice were retroorbitally bled 5 to 6 weeks post transplantation and stained with CD45.1-FITC, CD45.2-APC, Mac-1-PE, Gr-1-PE, CD3e-PE_Cy7 and CD45R/B220-APC_780 from eBioscience (CA, USA).

Colony forming unit assay

20,000 live cells were plated in triplicate from each tissue, grown in methylcellulose media (#MethoCult M3434, STEMCELL Technologies, BC, Canada) and maintained in mini-humidity chambers in 20% or 3% oxygen tissue culture incubators. Colonies were counted within two weeks of plating and identified based on morphology.

Statistics

Two-way t-test and Kaplan-Meier analyses were performed to assess statistical difference. A factor was considered statistically significant if it had a P-value of <0.05.

Supplementary Material

Refer to Web version on PubMed Central for supplementary material.

Acknowledgments

This work was supported by NIH grant CA82577 to Guillermina Lozano and the Cancer Center Support Grant to MDACC. We gratefully acknowledge Dr. Sean M. Post and Colby Suire for thoughtful discussions during the progress of this work and comments on the manuscript, and Emmanuelle Passegué for inspiring us to pursue this study. We would also like to thank Wendy Schober for technical assistance with flow cytometric analysis. M.J.Y. is supported by American Cancer Society Institutional Research Grant, Ladies Leukemia League, Institutional Research Grant and Physician Scientist Award of the University of Texas M. D. Anderson Cancer.

References

Bowie MB, McKnight KD, Kent DG, McCaffrey L, Hoodless PA, Eaves CJ. Hematopoietic stem cells proliferate until after birth and show a reversible phase-specific engraftment defect. The Journal of clinical investigation 2006;116:2808–2816. [PubMed: 17016561]

Brugarolas J, Bronson RT, Jacks T. p21 is a critical CDK2 regulator essential for proliferation control in Rb-deficient cells. The Journal of cell biology 1998;141:503–514. [PubMed: 9548727]

Chen Q, Fischer A, Reagan JD, Yan LJ, Ames BN. Oxidative DNA damage and senescence of human diploid fibroblast cells. Proceedings of the National Academy of Sciences of the United States of America 1995;92:4337–4341. [PubMed: 7753808]

Cheng T, Rodrigues N, Shen H, Yang Y, Dombkowski D, Sykes M, Scadden DT. Hematopoietic stem cell quiescence maintained by p21cip1/waf1. Science (New York, NY) 2000;287:1804–1808.

Collado M, Gil J, Efeyan A, Guerra C, Schuhmacher AJ, Barradas M, Benguria A, Zaballos A, Flores JM, Barbacid M, et al. Tumour biology: senescence in premalignant tumours. Nature 2005;436:642. [PubMed: 16079833]

Collado M, Serrano M. The power and the promise of oncogene-induced senescence markers. Nature reviews 2006;6:472–476.

Cosme-Blanco W, Shen MF, Lazar AJ, Pathak S, Lozano G, Multani AS, Chang S. Telomere dysfunction suppresses spontaneous tumorigenesis in vivo by initiating p53-dependent cellular senescence. EMBO Rep 2007;8:497–503. [PubMed: 17396137]

Donald SP, Sun XY, Hu CA, Yu J, Mei JM, Valle D, Phang JM. Proline oxidase, encoded by p53-induced gene-6, catalyzes the generation of proline-dependent reactive oxygen species. Cancer Res 2001;61:1810–1815. [PubMed: 11280728]

Honda R, Tanaka H, Yasuda H. Oncoprotein MDM2 is a ubiquitin ligase E3 for tumor suppressor p53. FEBS Lett 1997;420:25–27. [PubMed: 9450543]

Ito K, Hirao A, Arai F, Matsuoka S, Takubo K, Hamaguchi I, Nomiyama K, Hosokawa K, Sakurada K, Nakagata N, et al. Regulation of oxidative stress by ATM is required for self-renewal of haematopoietic stem cells. Nature 2004;431:997–1002. [PubMed: 15496926]

Ito K, Hirao A, Arai F, Takubo K, Matsuoka S, Miyamoto K, Ohmura M, Naka K, Hosokawa K, Ikeda Y, et al. Reactive oxygen species act through p38 MAPK to limit the lifespan of hematopoietic stem cells. Nature medicine 2006;12:446–451.

Jackson JG, Pereira-Smith OM. p53 is preferentially recruited to the promoters of growth arrest genes p21 and GADD45 during replicative senescence of normal human fibroblasts. Cancer Res 2006;66:8356–8360. [PubMed: 16951143]

Jang YY, Sharkis SJ. A low level of reactive oxygen species selects for primitive hematopoietic stem cells that may reside in the low-oxygenic niche. Blood 2007;110:3056–3063. [PubMed: 17595331]

Jones SN, Roe AE, Donehower LA, Bradley A. Rescue of embryonic lethality in Mdm2-deficient mice by absence of p53. Nature 1995;378:206–208. [PubMed: 7477327]

Kiel MJ, Yilmaz OH, Iwashita T, Yilmaz OH, Terhorst C, Morrison SJ. SLAM family receptors distinguish hematopoietic stem and progenitor cells and reveal endothelial niches for stem cells. Cell 2005;121:1109–1121. [PubMed: 15989959]

Kim I, He S, Yilmaz OH, Kiel MJ, Morrison SJ. Enhanced purification of fetal liver hematopoietic stem cells using SLAM family receptors. Blood 2006;108:737–744. [PubMed: 16569764]

Ko LJ, Prives C. p53: puzzle and paradigm. Genes & development 1996;10:1054–1072. [PubMed: 8654922]

Lee SH, DeJong J. Microsomal GST-I: genomic organization, expression, and alternative splicing of the human gene. Biochim Biophys Acta 1999;1446:389–396. [PubMed: 10524215]

Lehar SM, Nacht M, Jacks T, Vater CA, Chittenden T, Guild BC. Identification and cloning of EI24, a gene induced by p53 in etoposide-treated cells. Oncogene 1996;12:1181–1187. [PubMed: 8649819]

Li PF, Dietz R, von Harsdorf R. p53 regulates mitochondrial membrane potential through reactive oxygen species and induces cytochrome c-independent apoptosis blocked by Bcl-2. EMBO J 1999;18:6027–6036. [PubMed: 10545114]

Liu Y, Elf SE, Miyata Y, Sashida G, Liu Y, Huang G, Di Giandomenico S, Lee JM, Deblasio A, Menendez S, et al. p53 regulates hematopoietic stem cell quiescence. Cell Stem Cell 2009;4:37–48. [PubMed: 19128791]

Liu G, Parant JM, Lang G, Chau P, Chavez-Reyes A, El-Naggar AK, Multani A, Chang S, Lozano G. Chromosome stability, in the absence of apoptosis, is critical for suppression of tumorigenesis in Trp53 mutant mice. Nature genetics 2004;36:63–68. [PubMed: 14702042]

Liu G, Terzian T, Xiong S, Van Pelt CS, Audiffred A, Box NF, Lozano G. The p53-Mdm2 network in progenitor cell expansion during mouse postnatal development. The Journal of pathology 2007;213:360–368. [PubMed: 17893884]

Liu J, Cao L, Chen J, Song S, Lee IH, Quijano C, Liu H, Keyvanfar K, Chen H, Cao LY, et al. Bmi1 regulates mitochondrial function and the DNA damage response pathway. Nature 2009;459:387–392. [PubMed: 19404261]

Lombard DB, Chua KF, Mostoslavsky R, Franco S, Gostissa M, Alt FW. DNA repair, genome stability, and aging. Cell 2005;120:497–512. [PubMed: 15734682]

Ludwig RL, Bates S, Vousden KH. Differential activation of target cellular promoters by p53 mutants with impaired apoptotic function. Molecular and cellular biology 1996;16:4952–4960. [PubMed: 8756654]

Marine JC, Francoz S, Maetens M, Wahl G, Toledo F, Lozano G. Keeping p53 in check: essential and synergistic functions of Mdm2 and Mdm4. Cell Death Differ 2006;13:927–934. [PubMed: 16543935]

McDonnell TJ, Montes de Oca Luna R, Cho S, Amelse LL, Chaves-Reyes A, Lozano G. Loss of one but not two *mdm2* null alleles alters the tumor spectrum in *p53* null mice. J of Path 1999;188:322–328. [PubMed: 10419603]

Mendrysa SM, McElwee MK, Michalowski J, O'Leary KA, Young KM, Perry ME. mdm2 Is critical for inhibition of p53 during lymphopoiesis and the response to ionizing irradiation. Molecular and cellular biology 2003;23:462–472. [PubMed: 12509446]

Montes de Oca Luna R, Wagner DS, Lozano G. Rescue of early embryonic lethality in mdm2-deficient mice by deletion of p53. Nature 1995;378:203–206. [PubMed: 7477326]

Morrison SJ, Weissman IL. The long-term repopulating subset of hematopoietic stem cells is deterministic and isolatable by phenotype. Immunity 1994;1:661–673. [PubMed: 7541305]

Muller-Sieburg CE, Whitlock CA, Weissman IL. Isolation of two early B lymphocyte progenitors from mouse marrow: a committed pre-pre-B cell and a clonogenic Thy-1-lo hematopoietic stem cell. Cell 1986;44:653–662. [PubMed: 2868799]

Naka K, Muraguchi T, Hoshii T, Hirao A. Regulation of reactive oxygen species and genomic stability in hematopoietic stem cells. Antioxid Redox Signal 2008;10:1883–1894. [PubMed: 18627347]

O'Leary KA, Mendrysa SM, Vaccaro A, Perry ME. Mdm2 regulates p53 independently of p19(ARF) in homeostatic tissues. Molecular and cellular biology 2004;24:186–191. [PubMed: 14673154]

Orkin SH, Zon LI. Hematopoiesis: an evolving paradigm for stem cell biology. Cell 2008;132:631–644. [PubMed: 18295580]

Owusu-Ansah E, Banerjee U. Reactive oxygen species prime Drosophila haematopoietic progenitors for differentiation. Nature 2009;461:537–541. [PubMed: 19727075]

Palis J, McGrath KE, Kingsley PD. Initiation of hematopoiesis and vasculogenesis in murine yolk sac explants. Blood 1995;86:156–163. [PubMed: 7795222]

Palis J, Robertson S, Kennedy M, Wall C, Keller G. Development of erythroid and myeloid progenitors in the yolk sac and embryo proper of the mouse. Development (Cambridge, England) 1999;126:5073–5084.

Passegue E, Jamieson CH, Ailles LE, Weissman IL. Normal and leukemic hematopoiesis: are leukemias a stem cell disorder or a reacquisition of stem cell characteristics? Proceedings of the National Academy of Sciences of the United States of America 2003;100(Suppl 1):11842–11849. [PubMed: 14504387]

Polyak K, Xia Y, Zweier JL, Kinzler KW, Vogelstein B. A model for p53-induced apoptosis. Nature 1997;389:300–305. [PubMed: 9305847]

Post SM, Quintas-Cardama A, Terzian T, Smith C, Eischen CM, Lozano G. p53-dependent senescence delays Emu-myc-induced B-cell lymphomagenesis. Oncogene. 2009

Ringshausen I, O'Shea CC, Finch AJ, Swigart LB, Evan GI. Mdm2 is critically and continuously required to suppress lethal p53 activity in vivo. Cancer Cell 2006;10:501–514. [PubMed: 17157790]

Rowan S, Ludwig RL, Haupt Y, Bates S, Lu X, Oren M, Vousden KH. Specific loss of apoptotic but not cell-cycle arrest function in a human tumor derived p53 mutant. EMBO J 1996;15:827–838. [PubMed: 8631304]

Sharpless NE, Bardeesy N, Lee KH, Carrasco D, Castrillon DH, Aguirre AJ, Wu EA, Horner JW, DePinho RA. Loss of p16Ink4a with retention of p19Arf predisposes mice to tumorigenesis. Nature 2001;413:86–91. [PubMed: 11544531]

Terzian T, Wang Y, Van Pelt CS, Box NF, Travis EL, Lozano G. Haploinsufficiency of Mdm2 and Mdm4 in tumorigenesis and development. Molecular and cellular biology 2007;27:5479–5485. [PubMed: 17526734]

Vazquez A, Bond EE, Levine AJ, Bond GL. The genetics of the p53 pathway, apoptosis and cancer therapy. Nat Rev Drug Discov 2008;7:979–987. [PubMed: 19043449]

Weissman IL, Shizuru JA. The origins of the identification and isolation of hematopoietic stem cells, and their capability to induce donor-specific transplantation tolerance and treat autoimmune diseases. Blood 2008;112:3543–3553. [PubMed: 18948588]

Yamaoka A, Kuwabara I, Frigeri LG, Liu FT. A human lectin, galectin-3 (epsilon bp/Mac-2), stimulates superoxide production by neutrophils. J Immunol 1995;154:3479–3487. [PubMed: 7897228]

Zafon C. Jekyll and Hyde, the p53 protein, pleiotropics antagonisms and the thrifty aged hypothesis of senescence. Medical hypotheses 2007;68:1371–1377. [PubMed: 17166668]

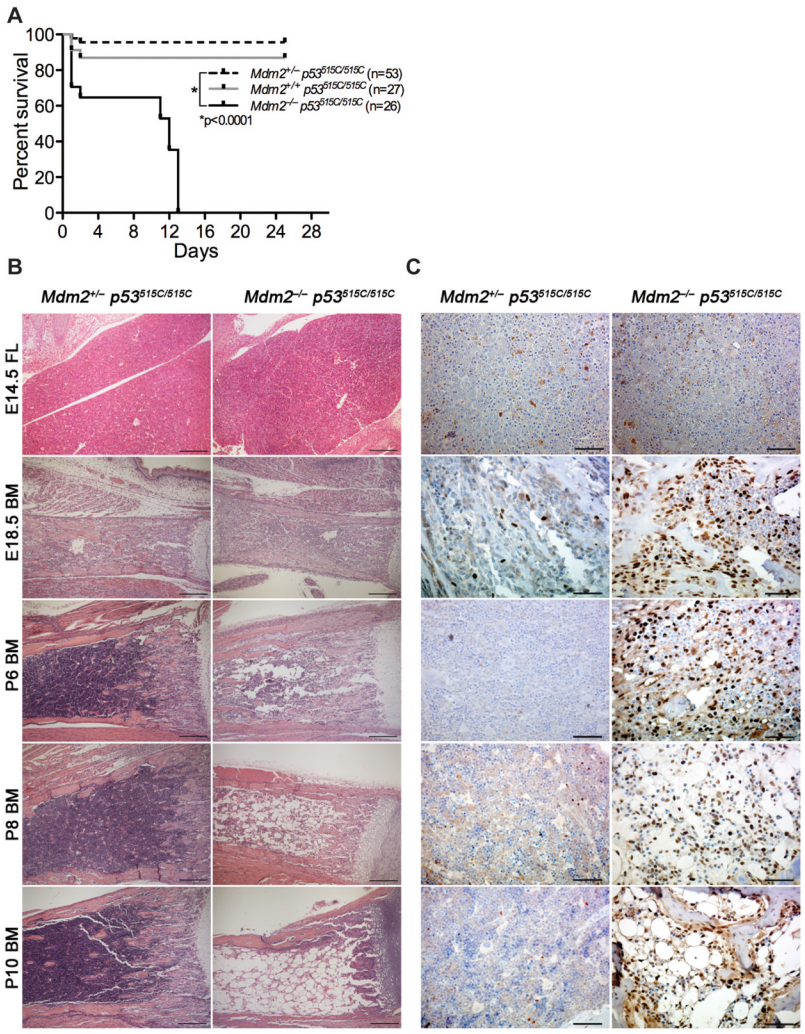

Figure 1. *Mdm2*$^{-/-}$ *p53*$^{515C/515C}$ mice die postnatally due to hematopoietic failure

(A) Kaplan-Meier survival curves of *Mdm2*$^{-/-}$ *p53*$^{515C/515C}$, *Mdm2*$^{+/-}$*p53*$^{515C/515C}$ and *Mdm2*$^{+/+}$ *p53*$^{515C/515C}$ mice. (B) Representative H&E staining of fetal livers (FL) at E14.5 and bone marrows (BM) at E18.5, P6, P8 and P10 from *Mdm2*$^{+/-}$*p53*$^{515C/515C}$ (left) and *Mdm2*$^{-/-}$ *p53*$^{515C/515C}$ mice (right). Scale bar is 200μm (C) Immunohistochemical staining of p53R172P on paraffin-embedded sections of E14.5 fetal livers, and E18.5, P6, P8 and P10 bone marrows from *Mdm2*$^{+/-}$*p53*$^{515C/515C}$ (left) and *Mdm2*$^{-/-}$ *p53*$^{515C/515C}$ (right). Scale bar is 50μm.

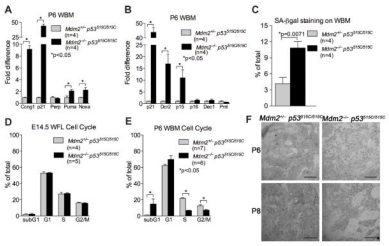

Figure 2. p53R172P transcriptional activity induces cell cycle arrest and senescence

(A) Expression levels of p53 regulated cell cycle (*Ccng1, p21*) and apoptosis (*Perp, Puma* and *Noxa*) genes were measured by Real Time RT-PCR from RNA of whole bone marrows (WBM) at P6 and were normalized to *Gapdh* levels. (B) Expression levels of senescence markers at P6 of whole bone marrow (WBM) RNA was measured by Real Time RT-PCR and was normalized to *Gapdh* levels. Sequences of primers used in A–B are listed in Supplementary Table 1. (C) Percent of SA-βgal positive cells of total P6-P8 whole bone marrows. (D–E) Cell cycle analysis of E14.5 whole fetal livers (WFL) (D) and P6 whole bone marrow (WBM) (E) using propidium iodide on fixed cells of these tissues. (F) Cleaved caspase-3 immunohistochemical staining on paraffin embedded bone marrows of $Mdm2^{+/-}p53^{515C/515C}$ (left) and $Mdm2^{-/-}\ p53^{515C/515C}$ (right) at P6 and P8. Insert is positive control. Scale bar is 50μm. Error bars represent standard error of the mean. See also Figure S1.

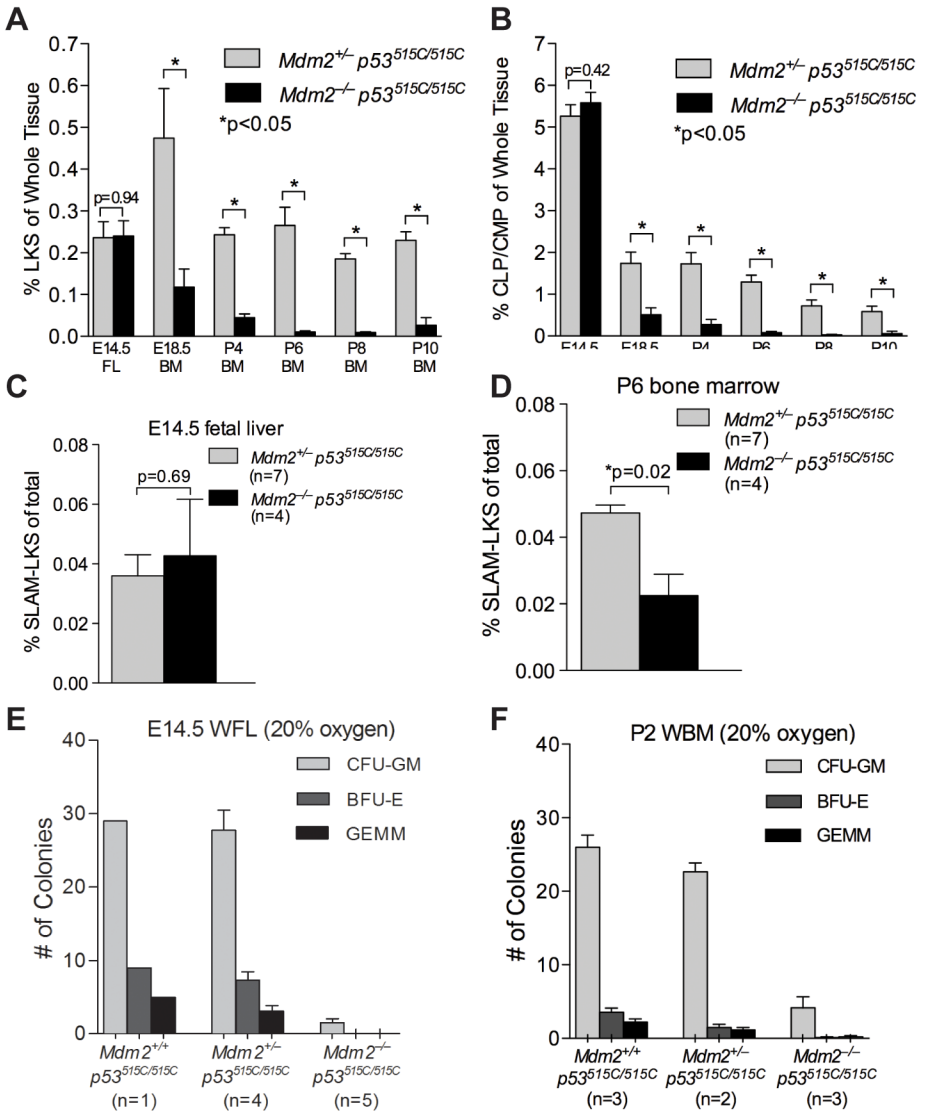

Figure 3. HSC and progenitors are not affected in fetal livers but ebb gradually after birth

(A) Percentage of LKS population of whole tissues from E14.5 fetal livers (FL), and E18.5, P4, P6, P8 and P10 bone marrows (BM). N>3 for all samples. (B) Percentages of CLP/CMP population of whole tissues from same time points as in (A). N>3 for all samples. (C–D) Percentage of SLAM-LKS cells of whole fetal liver at E14.5 (C) and whole bone marrow at P6 (D). (E–F) Quantification of CFU-GM, BFU-E and GEMM colonies from methocult cultures of 20,000 $Mdm2^{+/+}$ $p53^{515C/515C}$, $Mdm2^{+/-}p53^{515C/515C}$ and $Mdm2^{-/-}$ $p53^{515C/515C}$ whole fetal liver (WFL) cells (E) and whole bone marrow (WBM) (F) cells at E14.5 and P2, respectively. Error bars represent standard error of the mean. See also Figure S2.

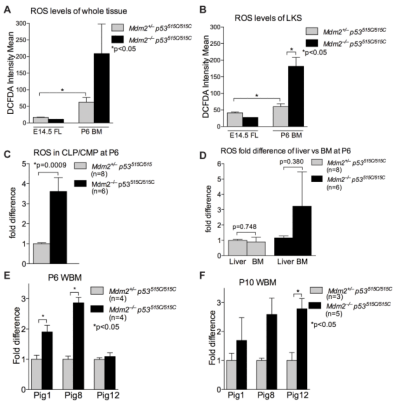

Figure 4. Increased ROS levels in postnatal bone marrows of *Mdm2*$^{-/-}$ *p53*$^{515C/515C}$ mice

(A) ROS levels were measured in whole tissues (fetal livers (FL) and bone marrows (BM) at E14.5 and P6 using DCFDA intensity as a readout. (B) Measurement of ROS levels with DCFDA in LKS populations of E14.5 fetal liver (FL) and P6 bone marrow (BM). See also Figure S3. (C) ROS in CLP/CMP in P6 bone marrows. Fold difference is relative to ROS levels of CLP/CMP of *Mdm2*$^{+/-}$*p53*$^{515C/515C}$ pups. (D) Measurement of ROS levels in whole liver and whole bone marrows in P6 pups. ROS levels of *Mdm2*$^{+/-}$*p53*$^{515C/515C}$ whole livers were set to 1. (E–F) Measurement of transcript levels of *Pig1*, *Pig8* and *Pig12* from whole bone marrow (WBM) cells at P6 (E) and P10 (F) from *Mdm2*$^{-/-}$ *p53*$^{515C/515C}$ compared to *Mdm2*$^{+/-}$*p53*$^{515C/515C}$ measured by Real Time RT-PCR and normalized to *Gapdh* levels. Error bars represent standard error of the mean.

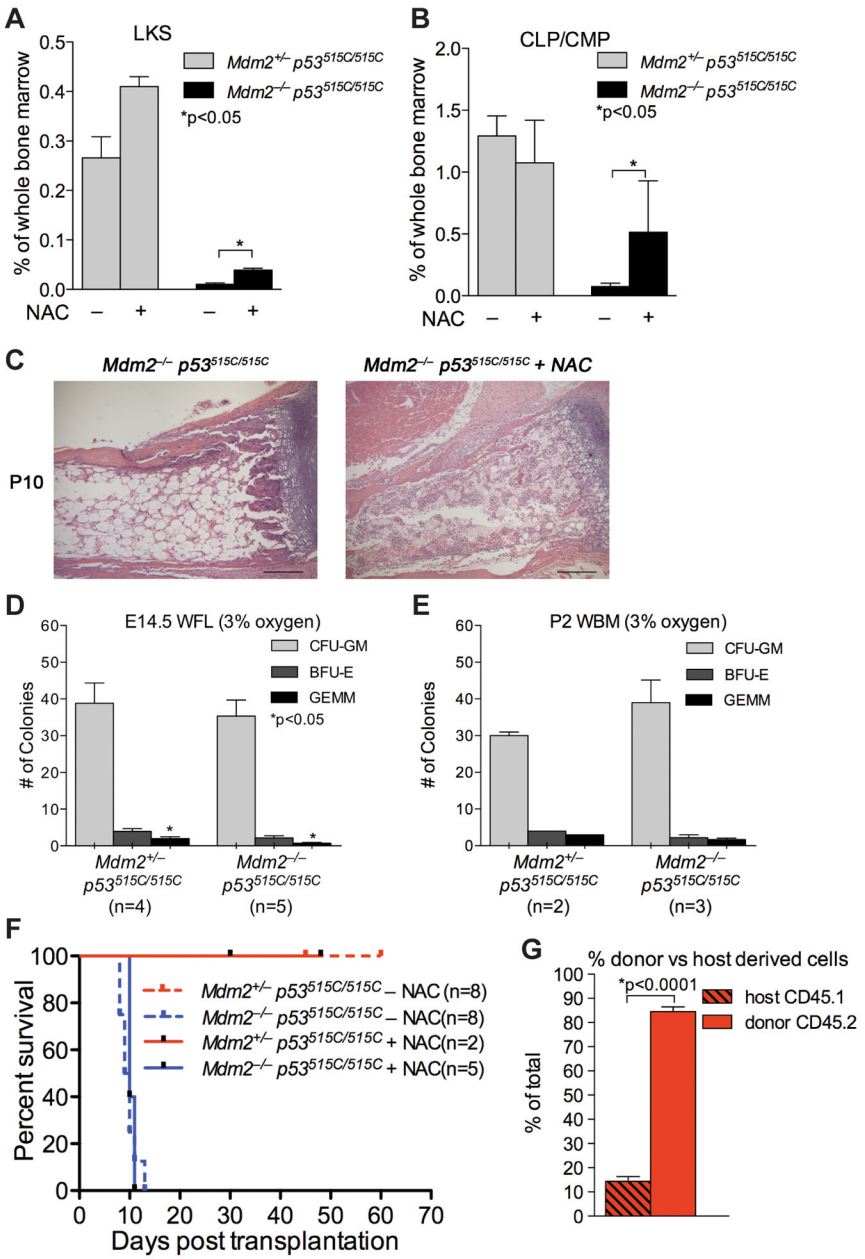

Figure 5. Rescue of hematopoietic defects upon treatment with NAC or culturing at 3% oxygen

(A–B) LKS (A) and CLP/CMP (B) populations of whole bone marrows at P6 for NAC treated and untreated mice. (C) Representative H&E staining for P10 bone marrow of a $Mdm2^{-/-}$ $p53^{515C/515C}$ mouse treated with NAC (right) compared to untreated (left). Scale bar is 200μm. (D–E) 20,000 cells of $Mdm2^{+/-}p53^{515C/515C}$ and $Mdm2^{-/-}$ $p53^{515C/515C}$ whole fetal livers (WFL) and whole bone marrow (WBM) cells were cultured at 3% oxygen and the number of CFU-GM, BFU-E and GEMM colonies were quantified. (F) Survival curve of CD45.1 mice transplanted with 0.5×10^6 $Mdm2^{+/-}p53^{515C/515C}$ or $Mdm2^{-/-}$ $p53^{515C/515C}$ whole bone marrow cells, supplemented with or without NAC in drinking water. (G) Percent of donor derived CD45.2 cells from peripheral blood assay at 5–6 weeks after transplantation. Error bars represent standard error of the mean. See also Figure S4.

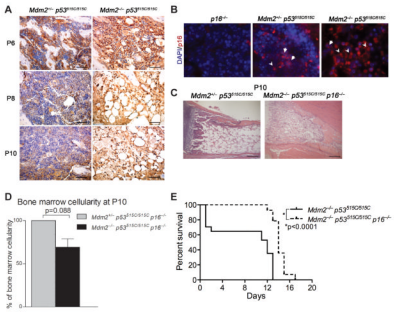

Figure 6. p16 is stabilized in *Mdm2*$^{-/-}$ *p53*$^{515C/515C}$ bone marrows and its loss rescues bone marrow cellularity

(A) Immunohistochemical staining of p16 in P6, P8 and P10 bone marrows of *Mdm2*$^{+-/}$*p53*$^{515C/515C}$ (left) and *Mdm2*$^{-/-}$ *p53*$^{515C/515C}$ (right) mice. Hematoxylin (blue) is nuclear counterstain. Scale bar is 50μm. (B) Immunofluorescence staining of P8 bone marrows for p16 using a different antibody than (A). Arrows indicate cytoplasmic or nuclear staining. (C) H&E staining of P10 bone marrows from *Mdm2*$^{-/-}$ *p53*$^{515C/515C}$ (left) and *Mdm2*$^{-/-}$ *p53*$^{515C/515C}$ p16$^{-/-}$ (right) mice. Scale bar is 200μm. (D) Percentage of bone marrow cellularity of *Mdm2*$^{-/-}$ *p53*$^{515C/515C}$ *p16*$^{-/-}$ mice compared to *Mdm2*$^{+-/}$*p53*$^{515C/515C}$ *p16*$^{-/-}$ littermates at P10. (E) Kaplan-Meier survival curve of *Mdm2*$^{-/-}$ *p53*$^{515C/515C}$ *p16*$^{-/-}$ mice (n=15) compared to *Mdm2*$^{-/-}$ *p53*$^{515C/515C}$ mice (n=26).

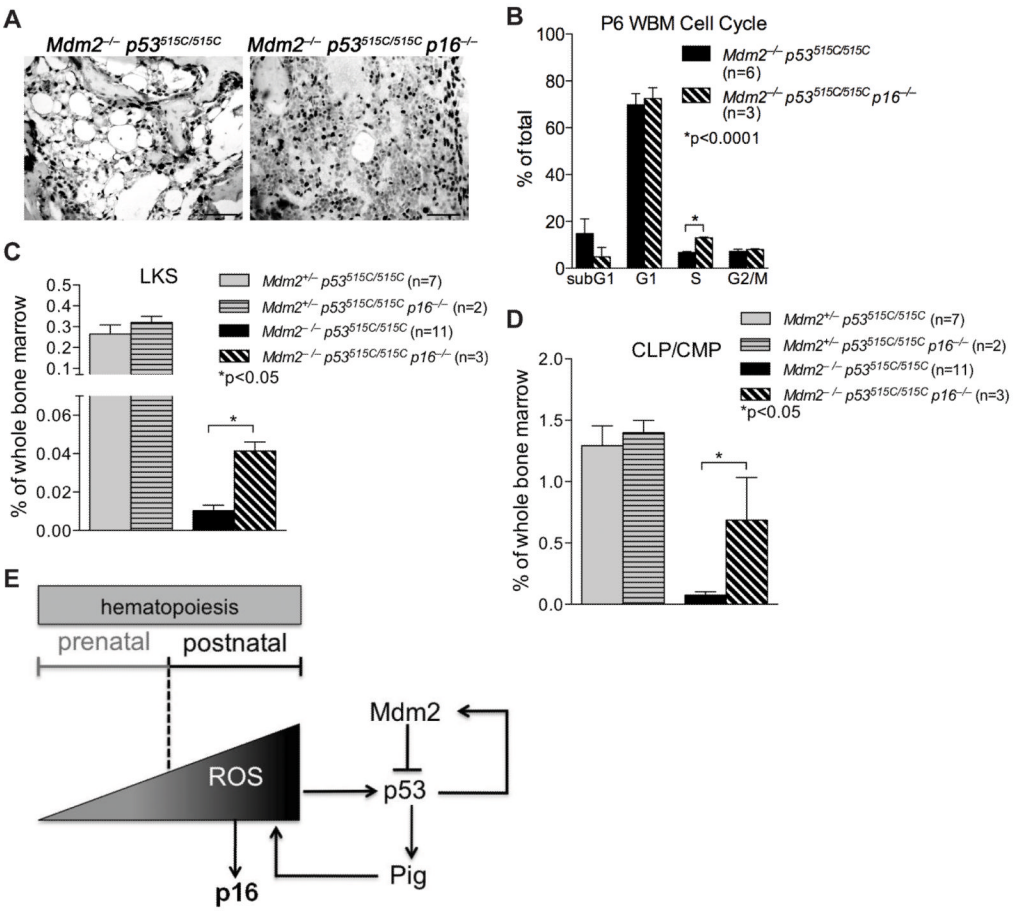

Figure 7. Partial rescue of LKS and CLP/CMP populations in *Mdm2*$^{-/-}$ *p53*$^{515C/515C}$ *p16*$^{-/-}$ mice

(A) p53R172P immunohistochemical analysis on P10 bone marrows (BM) of *Mdm2*$^{-/-}$ *p53*$^{515C/515C}$ (left) and *Mdm2*$^{-/-}$ *p53*$^{515C/515C}$ *p16*$^{-/-}$ (right) mice. Scale bar is 50μm. (B) Cell cycle status of P6 whole bone marrow cells (WBM) of *Mdm2*$^{-/-}$ *p53*$^{515C/515C}$ with and without *p16*. (C–D) LKS (C) and CLP/CMP (D) populations of P6 whole bone marrow of *Mdm2*$^{-/-}$ *p53*$^{515C/515C}$ *p16*$^{-/-}$ mice compared to *Mdm2*$^{-/-}$ *p53*$^{515C/515C}$ mice. (E) Suggested model for activation of p53 during hematopoiesis postnatally. Error bars represent standard error of the mean.